

The Characteristics of Square-Well Fluid Transport Coefficients

Dharmendra Kumar Dwivedee¹, K.K. Shukla², Dharmendra Pal^{3,*}

Abstract

The transport coefficients of the hard-sphere system were first computed by Alder, providing foundational insight into the microscopic origins of viscosity, diffusion, and thermal conductivity in simple fluids. Building on this framework, Evans derived a generalized Langevin equation to describe the time evolution of dynamical variables, incorporating memory effects and non-Markovian behavior in molecular motion. These theoretical developments established a bridge between microscopic interactions and macroscopic transport properties. When an attractive square-well potential is introduced in place of purely repulsive hard-sphere interaction, the system exhibits qualitatively distinct transport behavior. The attractive component significantly modifies collision dynamics, intermolecular correlations, and energy transfer processes. As the range and depth of the square-well potential increase, diffusion coefficients and shear viscosities display non-monotonic trends, reflecting competition between cohesive forces and kinetic mobility. Particularly at low to moderate densities, the addition of attractive interactions leads to substantial alterations in the characteristic transport coefficients, often producing enhanced dynamic heterogeneity and transient clustering effects. One of the most striking consequences is the observed breakdown of the Stokes-Einstein relation, which links self-diffusion to viscosity. In square-well fluids, this breakdown emerges at minimum densities and near the onset of liquid-like ordering, indicating a decoupling between molecular mobility and macroscopic resistance to flow. Such deviations underscore the limitations of classical transport models and highlight the importance of intermolecular attractions in determining the dynamic and rheological properties of dense and complex fluids.

Keywords: Liquids, behavior, measurements, hypotheses, potential

INTRODUCTION

The transport coefficients of liquids have been the subject of extensive study in recent years. The Chapman-Enskog theory has provided a comprehensive explanation for the transport properties of low-density gases [1], but the features of thick, stiff fluids have been mainly ignored. It is only very lately that kinetic and mode-coupling theories have provided an understanding of dense hard spheres with enough features for many different many-body systems [2–4]. These hypotheses are supported by neutron scattering measurements and computer models of hard-sphere-like fluids [5, 6], which show that important collision events associated with interatomic potentials are key.

The velocity-time correlation function (tcf) displays oscillating behavior for fluids with densities near the solid-liquid boundary, according to the investigation of hard-sphere fluids by Alder *et al.* [7]. Both Tang and Evans and Kirkpatrick found harmonic behavior in hard particles, and both studies determined the harmonic mode's frequency

*Author for Correspondence

Dharmendra Pal
E-mail: paldharmendra78@gmail.com

¹Research Scholar, Department of Physics, Maharishi University of Information Technology, Lucknow, Uttar Pradesh, India

²Professor Department of Physics, Maharishi University of Information Technology, Lucknow, Uttar Pradesh, India

³Senior Faculty, Department of Physics Department of Physics, St. Fidelis College, Lucknow, Uttar Pradesh, India

Received Date: October 04, 2025

Accepted Date: October 24, 2025

Published Date: November 15, 2025

Citation: Dharmendra Kumar Dwivedee, K.K. Shukla, Dharmendra Pal. The Characteristics of Square-Well Fluid Transport Coefficients. *Research & Reviews: Journal of Physics*. 2025; 14(3): 33–44p.

[8, 9]. While Tang and Evans discover that connected static and dynamic three-body correlations contribute to the oscillation frequency, Kirkpatrick attributes it to the fluid's static structural features. Consequently, there are a number of approaches that deal with correlated and uncorrelated collisions [10–15].

For non-spherical molecules, spin dynamics can be influenced by both correlated and uncorrelated collisions, according to Evans's investigation of the translational and rotational dynamics of ordinary fluids [14]. For a rigid spherical system, Evans calculated the correlation functions for self-diffusion, shear viscosity, and velocity-time assuming that friction is induced by both correlated backscattering (caging) collisions and uncorrelated binary collisions [15]. We shall stick to this method for the present undertaking.

According to Evans, the hard sphere concept does not account for attractive intermolecular interactions [15]. We examine the square-well fluid, where the velocity-time correlation function (tcf) of intermolecular interactions is affected by attracting and repulsive forces, to ensure consistency.

THEORY

Knowing the velocity-time correlation function (tcf) allows one to compute the transport coefficients, which in turn characterize the mass, momentum, and energy of a system. Applying the Green-Kubo relations in reference systems like the hard sphere becomes challenging due to the singularity in the temporal correlation function [16]. Their application in determining the integral of a limited-time correlation function and its transport coefficient remain ineffective in resolving the issue. This leads us to consider alternate methods, such as using the memory function instead of the velocity autocorrelation function.

The transport coefficients of the hard sphere system were computed by Alder *et al.* using the mean-square displacement method [7]. A generalized Langevin equation was derived by Evans by using Equation [15, 17].

$$\left(\frac{d}{dt}\right) C_v(t) = -f_E C_v(t) + \int_0^t d\tau R(t-\tau) C_v(\tau) \quad (1)$$

Where $C_v(t)$ is the velocity tcf,

$$C_v(t) = \frac{m}{3k_B T} \langle v \cdot v(t) \rangle \quad (2)$$

and m is the mass of the particle, and $k_B T$ is the thermal energy, f_E provides a representation of the Enskog friction drag that is produced by binary collisions that are not correlated, while $R(t)$ provides a representation of the memory function that is produced by events that are correlated. A formula may be found for the Enskog friction f_E , which is:

$$f_E = \frac{2}{3} \pi \sigma^2 g^{HS}(\sigma) V_F = \frac{2}{3} Z = \frac{16}{\sqrt{\pi}} \eta g^{HS}(\sigma) \omega$$

$$V_F = \sqrt{\frac{16k_B T}{\pi m}} \quad \text{and} \quad \omega = \sqrt{\frac{k_B T}{m \sigma^2}} \quad (3)$$

In this equation, Z represents the collision frequency per particle, v_F represents the relative thermal velocity, and $\eta = (\pi/6)\rho\sigma^3$ the proportion of the packing, and $g^{HS}(\sigma)$ is the rigid spherical fluid's contact pair correlation function, which may be approximated using the following form of the Carnahan and Starling equation:

$$g^{HS}(\sigma) = (1 - 0.5\eta)/(1 - \eta)^3. \quad (3.a)$$

σ is the Enskog friction drag as a result of binary collisions that are not correlated, and $R(t)$ means

the memory function, the result of correlated events. The Enskog friction, denoted as f_E , may be expressed as follows:

$$C_1(t) = \langle \delta(r - \sigma) P_1(r(t)) \delta(r(t) - \sigma) \rangle \quad (4)$$

According to the frequency-dependent memory function,

$$\tilde{R}(s) = \int_0^{\infty} dt \exp(-st) R(t) = -\Omega^2 \tilde{C}_1(s) \quad (5)$$

It is sufficient to just enter $t=0$ into the tcf in order to obtain an infinite. Tang and Evans discovered that the memory function may be obtained from its zero time value by using the following formula [9]:

$$R(t = 0^+) = -\Omega^2, \quad \Omega = \left(\frac{1}{4}\right) f_E \quad (5.a)$$

Ω to have been significant dynamical events involving three bodies. The potential expression for the velocity correlation function thereafter is [15]:

$$C_V(s) = \left(s + f_E + \frac{\Omega^2}{\omega} \tilde{h}_1(s) \right)^{-1} \quad (6)$$

Where,

$$\tilde{h}_1(s) = \frac{1}{1 + x + (1 + x)^{-1}}$$

with

$$x = \sqrt{\frac{s^2 \sigma^2}{2D(s)}}$$

Where $D(s)$ relates to the frequency-dependent diffusion coefficient. The following is a new way to define the diffusion coefficient:

$$D = \frac{k_B T}{m} \tilde{C}_V(s = 0) \quad (7)$$

$$\begin{aligned} \tilde{C}_V(s = 0) &= \left(0 + \frac{16}{\sqrt{\pi}} \eta g^{HS}(\sigma) \omega + \frac{16 \eta^2 [g^{HS}(\sigma)]^2 \omega \tilde{h}_1(s=0)}{\pi} \right)^{-1} \\ &= \left(0 + \frac{16}{\sqrt{\pi}} \eta g^{HS}(\sigma) \omega + \frac{16 \eta^2 [g^{HS}(\sigma)]^2 \omega \tilde{h}_1(s=0)}{\pi} \right)^{-1} \end{aligned} \quad (8)$$

On solving:

$$\tilde{h}_1(s = 0) = \left(\frac{1}{2}\right) \quad (9)$$

As a result, the diffusion coefficient may be solved mathematically as:

$$D = \left(\frac{k_B T}{m \sigma^2}\right)^{(1/2)} \sigma^2 \left(\frac{16}{\sqrt{\pi}} \eta g^{HS}(\sigma) + \frac{8 \eta^2 g^{2HS}(\sigma)}{\pi} \right)^{-1} \quad (10)$$

In addition, the reduced diffusion coefficient's final formula can be expressed in the same way as shown below:

$$\begin{aligned} D^{HS*} &= \frac{D}{(k_B T / m \sigma^2)^{(1/2)} \sigma^2} \\ &= \left(\frac{16 \eta g^{HS}(\sigma)}{\sqrt{\pi}} + \frac{8 \eta^2 g^{2HS}(\sigma)}{\pi} \right)^{-1} \end{aligned} \quad (11)$$

here $g^{HS}(\sigma)$.

The hard sphere system's pair correlation function is represented by this equation. The Chapman-Enskog technique of solution may be used to estimate the self-diffusion coefficient of a fluid contained in a square well [18, 19], for instance, by inserting the pair correlation function $g^{HS}(\sigma)$ in Eq. (11) by $g^{SQ}(\sigma)$ as:

$$g^{SQ}(\sigma) = g^{SW}(\sigma) + \lambda^2 g^{SW}(\lambda\sigma)E \quad (11)$$

Eq. (11) was similarly obtained by Longuet-Higgins and Valleau by supposing that a particle's velocity autocorrelation function decays exponentially with time [20]. Their research was carried out with this assumption. In order to obtain the achieved values, several actions were essential. Thus, in the case of self-diffusion, the results obtained using the Chapman-Enskog approach, the Longuet-Higgins method, and the Valleau method are identical. Applying the pair correlation function to fluids with square wells is the standard procedure $g^{SW}(\sigma)$ in a way that, using the high temperature approximation (HTA), might be stated as [21]:

$$g^{SW}(\sigma) = g^{HS}(\sigma) + \frac{1}{4T^*} \frac{\partial a_1^{SW}}{\partial \eta} + \frac{\lambda^3}{T^*} g^{HS}(\lambda\sigma) \quad (12)$$

where a_1^{SW} is the first-order disturbance term linked to attractive energy.

$$a_1^{SW} = -4\eta(\lambda^3 - 1) \left\{ \frac{1 - (\eta_{\text{eff}}/2)}{(1 - \eta_{\text{eff}})^3} \right\} \quad (13)$$

and

$$\eta_{\text{eff}} = C_1\eta + C_2\eta^2 + C_3\eta^3 \quad (14)$$

Matrices C1, C2, and C3 are provided by Gil-Villegas *et al.* [22]. The functions $g^{SW}(\sigma)$ and $g^{SW}(\lambda\sigma)$ are the radial distribution functions that may be defined as indicated by Yu *et al.* [23], and they are evaluated at the specified sites σ and $\lambda\sigma$, respectively.

$$g^{SW}(\lambda\sigma) = g^{HS}(\lambda\sigma) \exp\left(\frac{\alpha}{T^*} + \frac{\beta}{T^{*2}}\right) \quad (15)$$

Where, $T^* = k_B T / \varepsilon$.

After a thorough analysis, it was found that α was -0.4317 and β was -0.1177 . The hard sphere system's pair correlation function is represented by this equation. The self-diffusion coefficient of a fluid in a square well can be found, for instance, by using the Chapman-Enskog technique of solution to the pair correlation function [18, 19].

$$g^{HS}(\lambda\sigma) = 0.99948 + 0.82404\eta - 3.46976\eta^2 \quad (16)$$

It is possible to define the term E in Eq. (11) as:

$$E = \exp\left(\frac{\varepsilon}{kT}\right) - \left(\frac{\varepsilon}{2kT}\right) - 2J$$

Where J represents the function that is dependent on temperature as [22]:

$$J = \frac{0.5 + 0.28304/T^*}{1 + 0.15360/T^*}$$

A Stokes-Einstein relation is used to establish a connection between the shear viscosity and the diffusion coefficient ($2\pi FD\sigma/kBT = 1$).

This SE connection that Evans presented was utilized by us [25]:

$$(2\pi\eta_F^{SW} D^{SW}\sigma/k_B T = 1).$$

Also, we followed this SE link that Evans had supplied us. The outcomes predicted by the two assertions are identical [15]. The shear viscosity must be determined in this case, η_F^{SW} . Using Evans's suggested Stokes-Einstein relation, we have:

$$\frac{2\pi D^{SW}[\eta_F^{SW} - \eta_E]\sigma}{k_B T} = \frac{4\eta_E f_E}{25\omega(1+S)} \quad (17)$$

Where,

$$\frac{[\eta_F^{SW} - \eta_E]}{m\rho} = \frac{256\sigma^2(\eta g^{SQ}(\sigma))^2 \omega}{75\pi} \quad (18)$$

and

$$\frac{\eta_E}{m\rho} = \sigma^2 \omega Y \quad (19)$$

Where,

$$Y = \left\{ \frac{5\sqrt{\pi}}{96\eta g^{SQ}(\sigma)} \left(1 + \frac{8\eta g^{SQ}(\sigma)}{5} \right)^2 + \frac{8\eta g^{SQ}(\sigma)}{5\sqrt{\pi}} \right\} \quad (20)$$

The lower shear viscosity is the result of solving the problem η_F^{*SW} as:

$$2\pi D^{*SW} \eta_F^{*SW} = \frac{4\eta_E f_E}{25\omega(1+S)} + 12D^{*SW} \eta Y \quad (21)$$

where

$$\eta_F^{*SW} = \frac{\eta_E^{SW}}{(k_B T / m\sigma^2)^{1/2} m/\sigma} \quad (22)$$

and

$$S = \frac{f_E}{32\omega} = \frac{\eta g^{SQ}(\sigma)}{2\sqrt{\pi}} \quad (23)$$

We make a comparison between our findings and the concept that Nigra and Evans initially proposed in order to prove the reliability of our findings [25]. It is possible that the value that Nigra and Evans offered for the diffusion coefficient (in reduced units) has a solution is something that can be determined [25].

$$D_{Evans}^{SW} = \frac{3}{8\rho * \sqrt{\pi} g^{HS}(\sigma)[1 + 8\eta\lambda^3 g_1(\lambda\sigma) f^2 F]} \quad (24)$$

where $F = (7\lambda^3 + 2)/(42\lambda^3 - 7f\lambda^3 - 8f)$,

$$f = 1 - e^{-\epsilon/kT} = 1 - e^{-1/T^*}, g_1(\lambda\sigma) = e^{\epsilon/kT} = e^{1/T^*}.$$

The shear viscosity that Nigra and Evans proposed can be expressed as being able to be expressed in reduced units [25].

$$\eta_{Evans}^{SW} = \frac{8\rho * \sqrt{\pi}}{3} \left(\frac{g^{HS}(\sigma)}{2\pi} + \frac{4f^2 \pi \lambda^5 \rho^* g_1(\lambda\sigma) \bar{n}}{15} \right) \quad (25)$$

Where,

$$\bar{n} = \frac{11\lambda^5 + 4}{11(10 - f)\lambda^5 - 24f}$$

$$\rho^* = \rho\sigma^3.$$

Through the utilization of the SE relation, it is possible to get the shear viscosity (in reduced units) from Eq. (24).

$$\eta_{SE}^{*SW} = \frac{4\rho^* g^{HS}(\sigma)}{3\sqrt{\pi}} (1 + 8\eta\lambda^3 g_1(\lambda\sigma) f^2 F) \quad (26)$$

DISCUSSION AND RESULTS

Due to the fact that it is one of the most straightforward fluid models, the square-well fluid is able to accurately depict the fundamental behavior of interactions between hard spheres. As a result, it is an appropriate model for modeling liquids. The square-well model was initially utilized by Longuet-Higgins and Vallea in order to provide a description of the self-diffusion coefficients of thick fluids [20]. The DRS hypothesis, which is analogous to the Enskog hard sphere (EHS) theory, was created by Davis *et al.* with the intention of gaining a better understanding of the transport coefficients of square-well fluids [18]. In addition, Wilbertz developed a kinetic theory in order to ascertain the self-diffusion coefficients of square-well fluids. The outcomes of their theoretical predictions were validated through the use of computer simulations. In spite of this, the WMBL hypothesis argues that reliable forecasts are restricted to concentrations that are about moderate.

When it comes to accounting for the intricacy of multi-body interactions and the short period of collisions, the kinetic theory of transport mechanisms has encountered a number of obstacles. In spite of this, a great number of novel models have been created in order to offer formulations of the self-diffusion coefficient for hard-sphere systems that are more precise [9–15]. An example of such a theory is offered by Evans, which computes the velocity time correlation function for a system that is rigid and spherical [15]. After that, the self-diffusion coefficient and the shear viscosity of a fluid that is contained within a square well may be calculated with the help of this function.

The radial distribution function at contact, which indicates where the centers of two molecules meet during collision, is a defining feature of the square-well fluid under Chapman-Enskog theory. This feature largely accounts for the attractive properties of the square-well fluid. In this study, we examine this distinct characteristic by estimating the pair correlation function at contact using the high-temperature approximation [21, 22]. The factor η_{eff} used to calculate the mean attractive energy plays a crucial role in determining the transport properties. The numerical results presented in this study are expressed in reduced units.

Figure 1 displays case-specific molecular dynamics results and the reduced self-diffusion coefficients obtained from Eq. (11). The values of T (reduced temperature) are 2, 3, and 5, while λ (well width) is set at 1.5. Using $g^{HS}(\sigma)$ and Eq. (11), we derive D^{HSx} as shown in Figure 1. Additionally, we calculate the self-diffusion coefficient D using the Smoluchowski equations for pair diffusion with an effective two-body intermolecular force, based on the square-well potential formula by Nigra and Evans [25]. For $\lambda = 1.5$ and $T^* = 2, 3,$ and 5, the results of this study are compared to molecular dynamics (MD) data in Figures 2–4. The proposed method yields results that are in strong agreement with Nigra and Evans' expression at medium and high densities, though a slight discrepancy is noted at low densities [25]. This disparity may arise because the present formula is tailored for dense fluids.

Figure 5 illustrates the experimentally measured relationship between density, well depth, and the square-well fluid's reduced shear viscosity with $\lambda = 2.5$. Shear viscosity increases with density, while diffusivity decreases, regardless of whether the well depth ($T^* - 1$) is increasing or decreasing. Discrepancies between low-density diffusivity and molecular dynamics results may stem from the focus on dense fluids in the theoretical transport coefficient formulation [15]. For highly viscous fluids, it is assumed that the memory function remains constant over time.

Figure 1 shows the diffusivity of a system using dotted lines to represent hard spheres. At low and intermediate densities, adding a square-well to hard spheres reduces diffusion, while at high densities, it has no impact. This can be explained by the square-well increasing the cross-section of the particles, causing more scattering and reducing diffusivity. If a well potential disrupts the negative temporal correlation at high densities, diffusivity may increase. Figures 1–5 also show that, unlike in previous harmonic models, shear viscosity is finite, and the diffusion coefficient remains present [8, 9].

Lastly, Figure 6 validates the Stokes-Einstein relation for a square-well fluid, demonstrating its temperature dependence at low densities. However, the relation approaches unity at high densities, behaving like a hard-sphere system at medium and high densities due to its temperature dependence.

Additionally, it is observed that when the product is at lower densities, $\eta^{*SW}_F D^{*SW}$ with increasing well depth, it has a tendency to vary to much lower values ε^* (i.e., T^{*-1}). As will become clear in the next paragraphs, molecular dynamics data corroborate this. Identical conditions, the diffusion coefficient for hard spheres is greater than that for square-well systems. Furthermore, as the hole depth increases, the diffusion coefficient drops for materials with low densities. This happens as the depth of the well is raised. Furthermore, it has been shown that the diffusion coefficient variation is more significant than the shear viscosity fluctuation [25]. The purpose of this experiment was to test the viability of the Stokes-Einstein connection at low-temperature applications. Because they are both derived from the same set of parameters, Nigra and Evans were able to generate both the shear viscosity and the diffusion coefficient formulations [25].

$$\varepsilon^* = 0.5 \text{ or } T^* = 2.0$$

$$\rho^* \lambda = 1.4 \quad \lambda = 1.5 \quad \lambda = 1.6$$

Continued work by MD

0.2	0.526	0.664	0.518	0.628	0.503	0.598
0.4	0.232	0.265	0.225	0.247	0.213	0.236
0.6	0.116	0.114	0.109	0.106	0.100	0.102
0.8	0.050	0.039	0.045	0.039	0.042	–
0.86	0.037	0.025	0.033	0.026	0.031	–
0.90	0.029	0.002	0.027	0.020	0.025	–

Figure 1 demonstrates the lower self-diffusion coefficients of a square-well fluid as a function of the reduced density of the fluid under consideration. At reduced temperatures $T^* = 2, 3,$ and 5 . For clarity, the Y-axis has been shifted by $+0.2$ units for $T^* = 3$ and by $+0.4$ units for $T^* = 5$. The dotted line represents the reduced diffusion coefficient for a hard sphere fluid. Molecular dynamics (MD) simulation results are indicated by symbols for each temperature: for $T^* = 2$, \diamond for $T^* = 3$, and \triangle for $T^* = 5$.

Figure 2 compares the present model to the one created by Nigra and Evans [25], drawing attention to the parallels and variations in how the two models anticipate the self-diffusion coefficients of a square-well fluid at a lowered temperature of $T^* = 2$. The two models are compared with respect to the patterns of decreasing self-diffusion coefficients, highlighting their commonalities and differences.

Figure 3 shows a comparison between the current model and the model proposed by Nigra and Evans [25] for finding the square-well fluid's lowered self-diffusion coefficients at a reduced temperature of $T^* = 3$. To find out how well either model predicts the fluid's self-diffusion behavior under these circumstances, we are comparing the two.

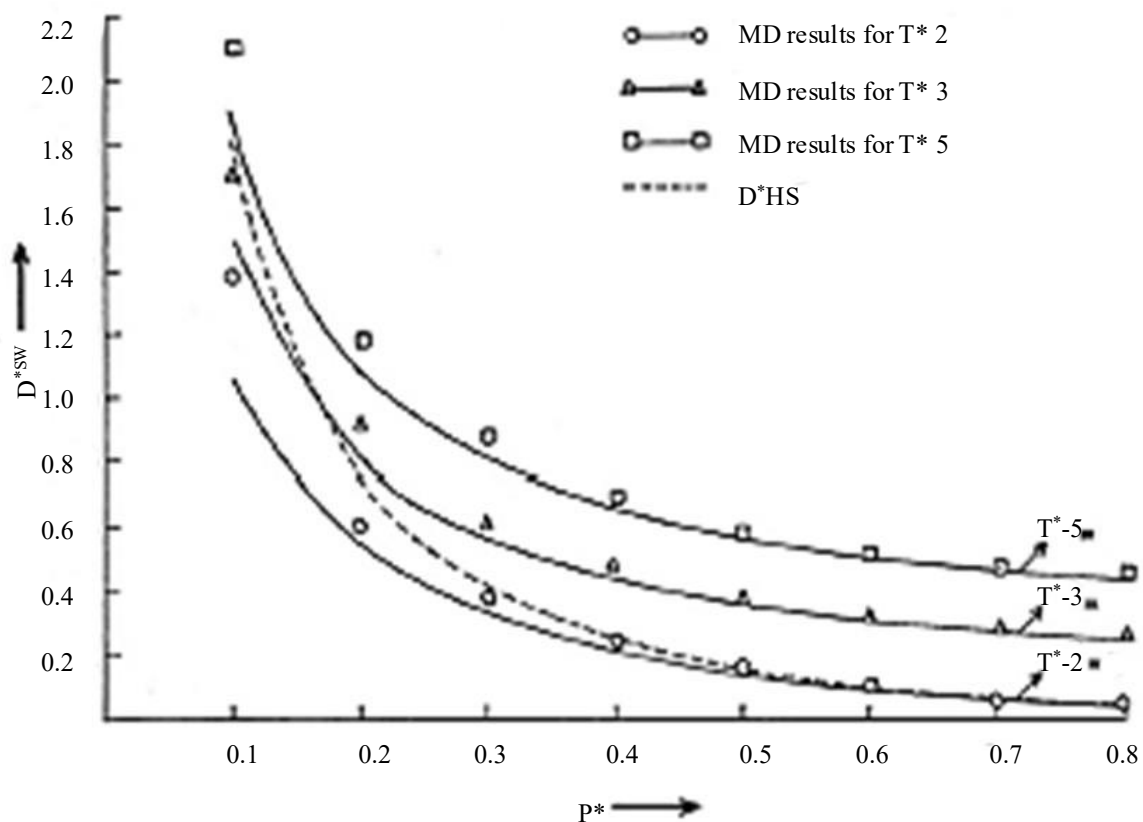


Figure 1. Diffusion coefficient variation with density for different model potentials.

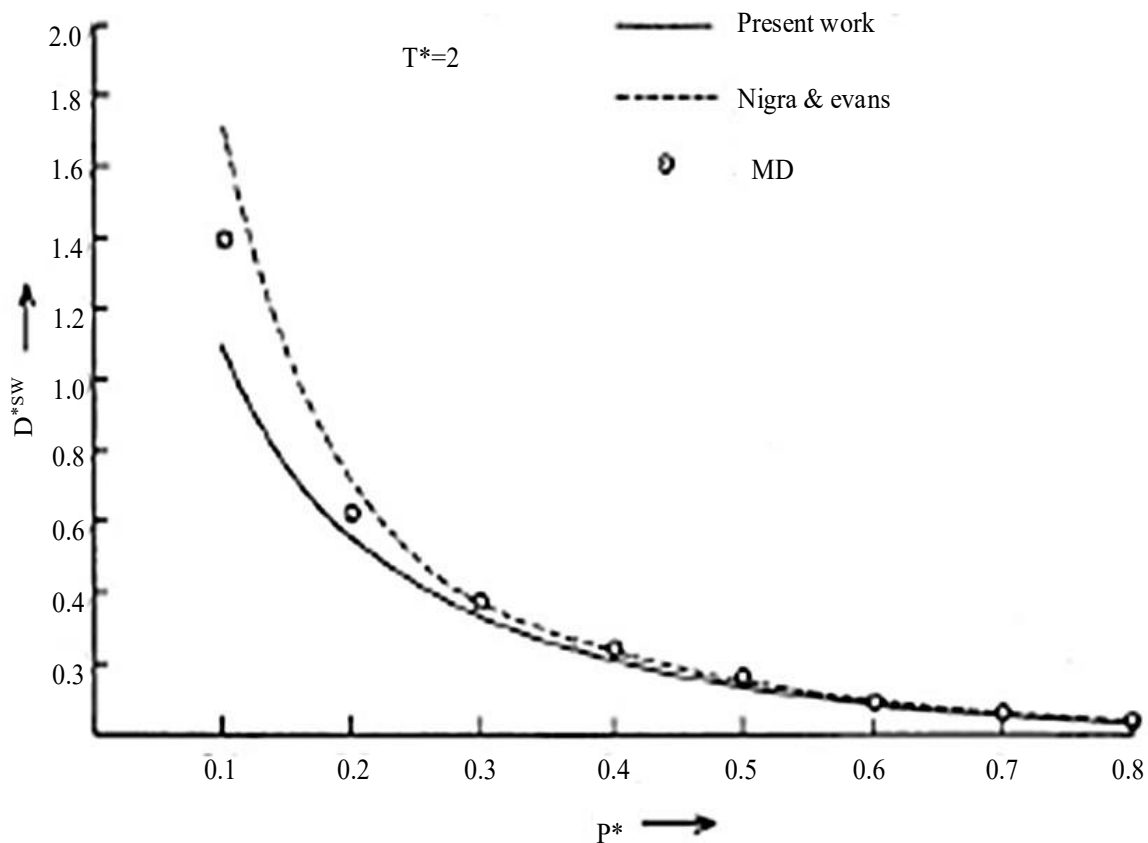


Figure 2. Open circles indicate molecular dynamics.

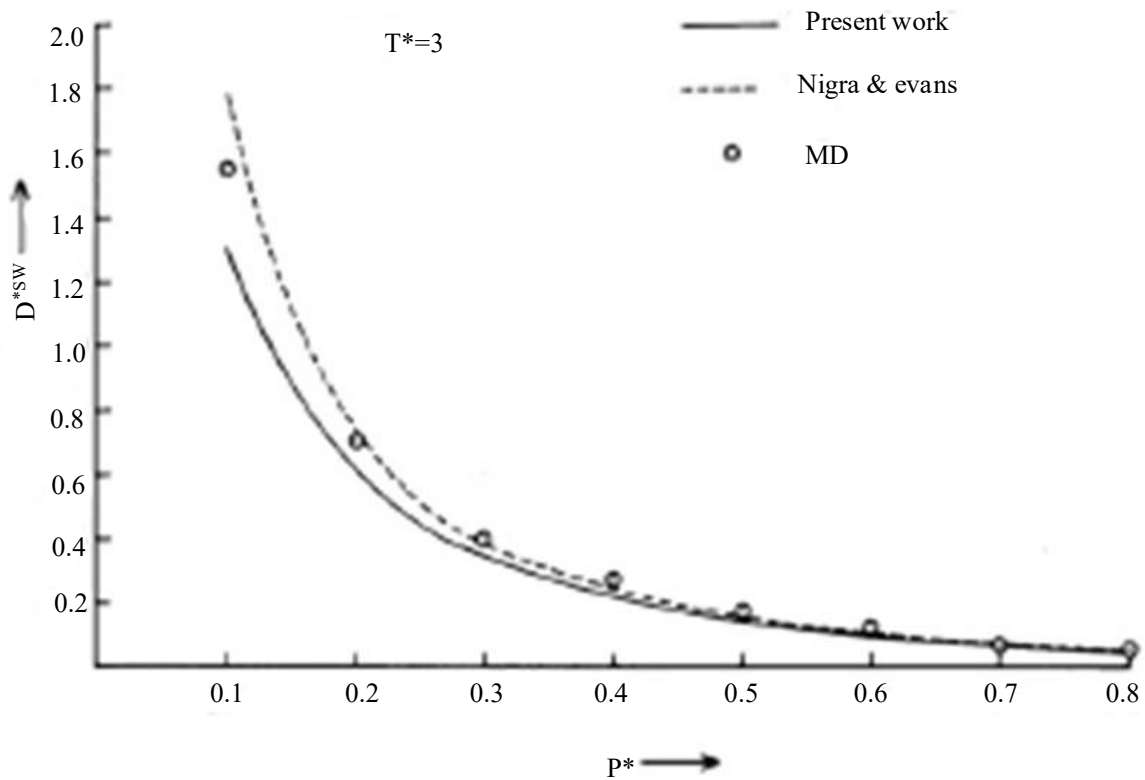


Figure 3. Reduced self-diffusion coefficient D_{sw}^* .

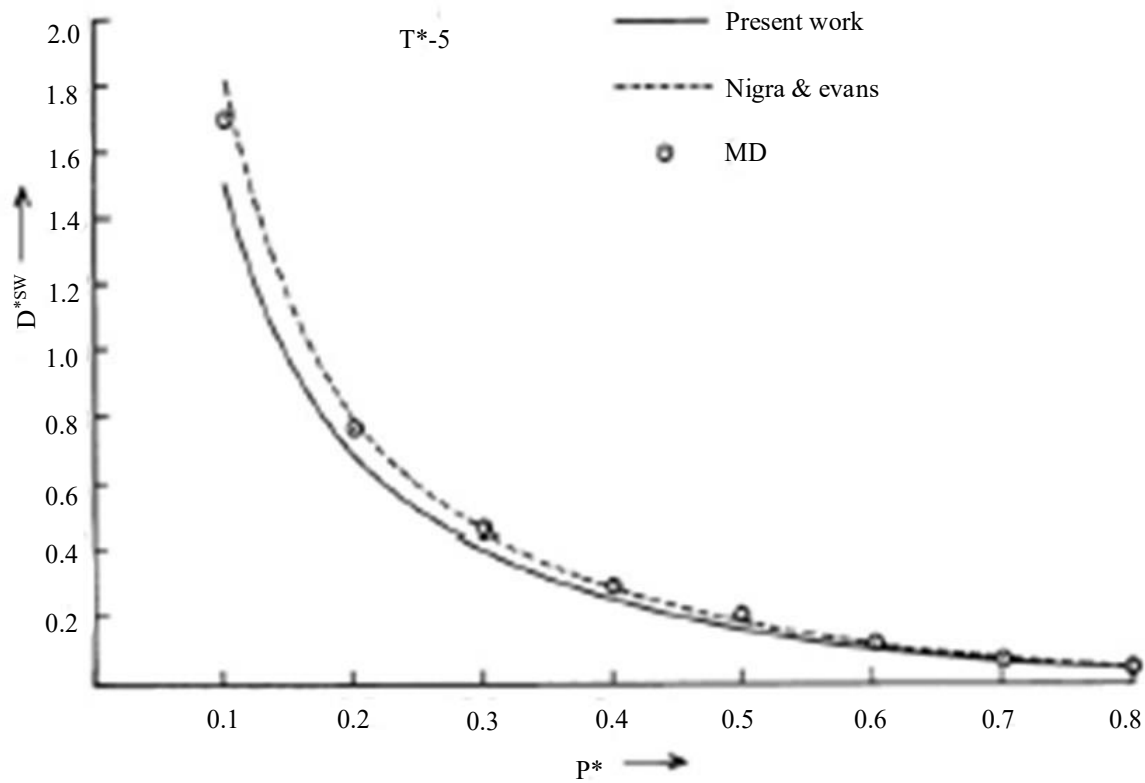


Figure 4. Comparison between the current model and the model.

Figure 4 draws comparisons between the current model and the one developed by Nigra and Evans [25], with the purpose of predicting the reduced self-diffusion coefficients of a square-well fluid at a

reduced temperature of $T^* = 5$. It contrasts and compares the present model with that of Nigra and Evans [25], in order to forecast the lowered self-diffusion coefficients of a square-well fluid at a reduced temperature as a function of reduced density ($\rho\sigma^3 = \rho^*$) for reduced temperatures $T^* = 2, 3$, and 5 . To enhance clarity, the Y-axis has been offset by +1 unit for $T^* = 3$ and by +2 units for $T^* = 5$. The decreased shear viscosity for a hard spherical fluid is seen by the dotted line. Results of molecular dynamics (MD) simulations are shown using several symbols for $T^* = 2$, \diamond for $T^* = 3$, and \triangle for $T^* = 5$. (Figure 5).

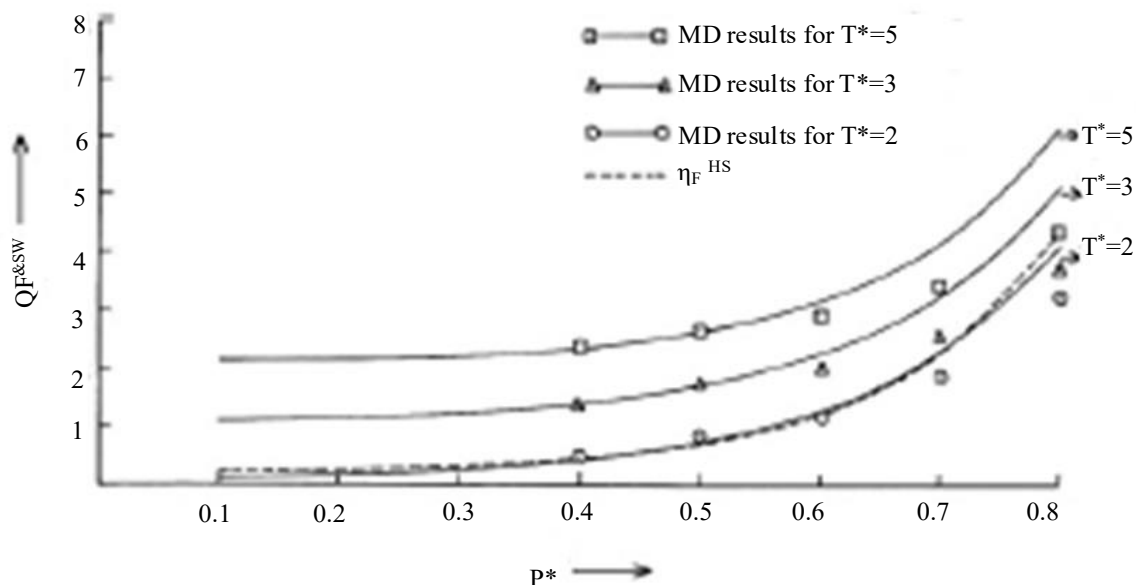


Figure 5. Illustrates the decreasing shear viscosity of a square-well fluid.

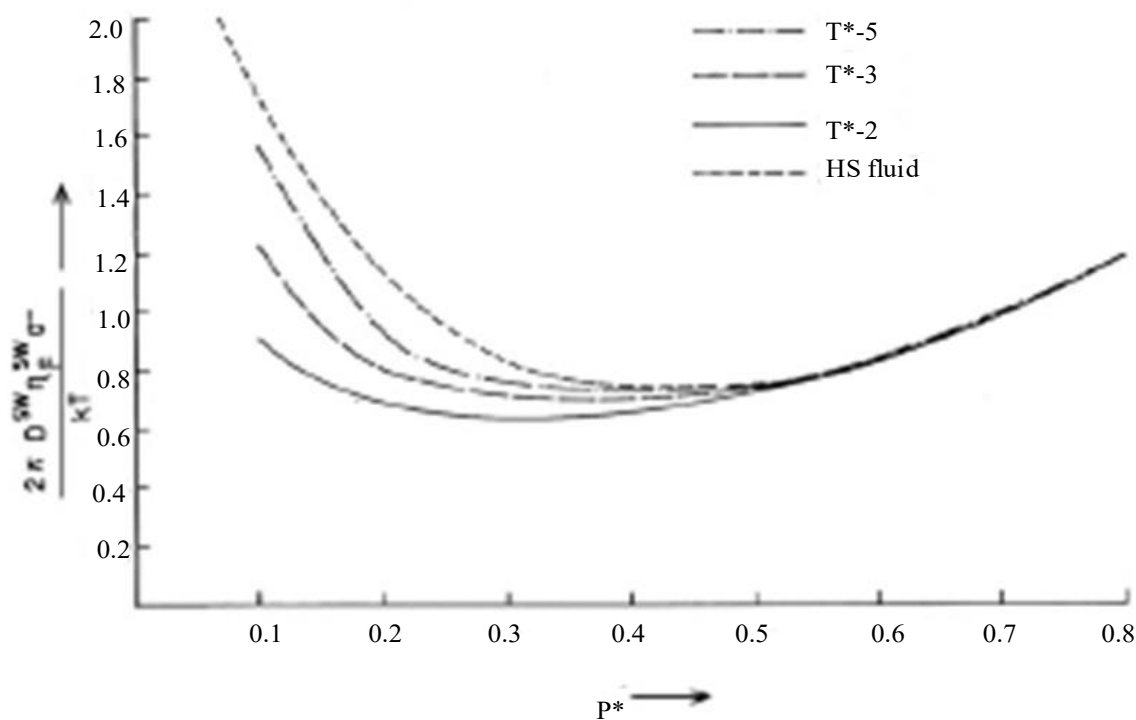


Figure 6. Uses a square-well fluid to investigate the Stokes-Einstein connection.

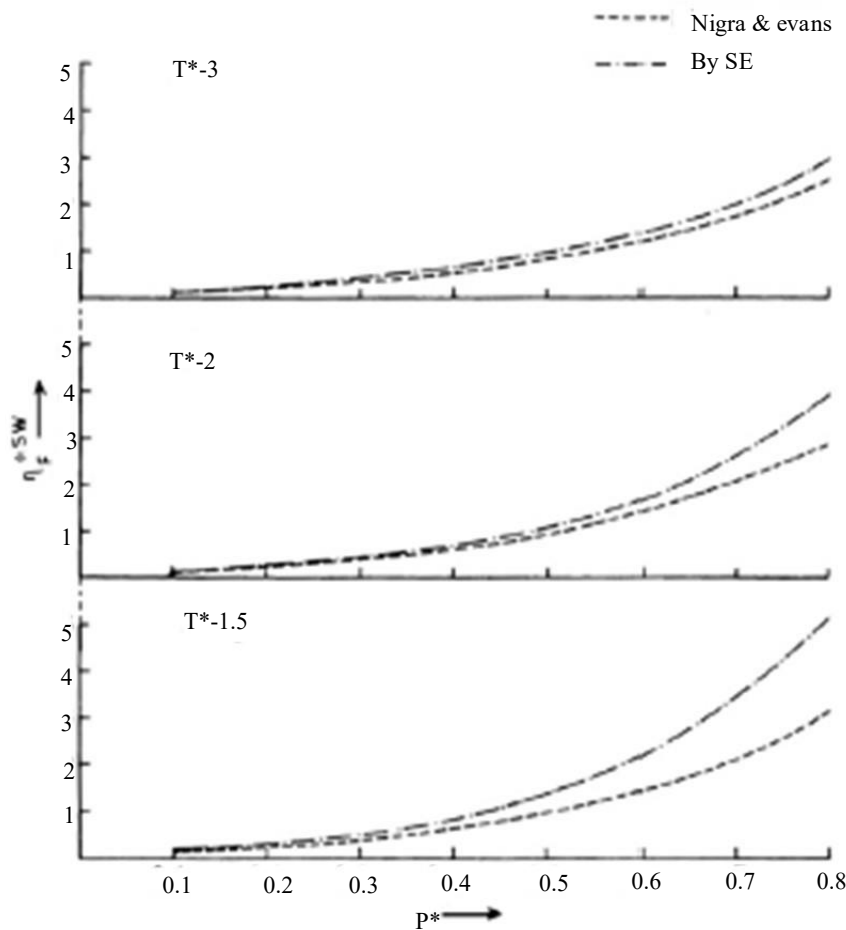


Figure 7. Evaluates the square-well fluid's decreased shear viscosity.

The solid line depicts to show this relation for a rigid spherical system $T^* = 2$, the large dashed line represents $T^* = 3$, and the dash-dotted line represents $T^* = 5$. There is a little dashed line that represents the Stokes-Einstein (SE) connection. Figure 6 compares it to the shear viscosity computed using the Stokes-Einstein relation, which is based on the Nigra and Evans model. At lower temperatures, the comparison is made $T^* = 3, 2, \text{ and } 1.5$. (Figure 7).

CONCLUSION

This model, which was provided by Evans, will function well regardless of whether the fluid is square-well or hard spherical. However, more modifications to its memory function are required, and these modifications have the potential to provide outcomes that conform to the findings that Nigra and Evans articulated for square-well fluids in our study.

REFERENCES

1. Chapman S, Cowling TG. The Mathematical Theory of Non-uniform Gases: An Account of the Kinetic Theory of Viscosity, Thermal Conduction and Diffusion in Gases. Cambridge: Cambridge University Press; 1990.
2. Balucani U, Zoppi M. Dynamics of the Liquid State. Oxford: Clarendon Press; 1995. doi:10.1093/oso/9780198517399.001.0001.
3. Bosse J, Götze W, Lücke M. Mode-coupling theory of simple classical liquids. Phys Rev A. 1978;17(1):434–446. doi:10.1103/PhysRevA.17.434.

4. Leutheusser E. Dynamics of a classical hard-sphere gas. II. Numerical results. *J Phys C*. 1982;15(13):2827–2843. doi:10.1088/0022-3719/15/13/012.
5. Alder BJ, Wainwright TE. Decay of the velocity autocorrelation function. *Phys Rev A*. 1970;1(1):18–21. doi:10.1103/PhysRevA.1.18.
6. Morkel C, Gronemeyer C, Gläser W, Bosse J. Experimental evidence for the long-time decay of the velocity-autocorrelation in liquid sodium. *Phys Rev Lett*. 1987;58:1873–1876. doi:10.1103/PhysRevLett.58.1873.
7. Alder BJ, Gass DM, Wainwright TE. Studies in molecular dynamics. VIII. The transport coefficients for a hard-sphere fluid. *J Chem Phys*. 1970;53(10):3813–3826. doi:10.1063/1.1673845.
8. Kirkpatrick TR. Does the velocity autocorrelation function oscillate in a hard-sphere crystal? *J Stat Phys*. 1989;57(3):483–496. doi:10.1007/BF01022818.
9. Tang S, Evans GT. Harmonic modes in a hard sphere fluid. *Phys Rev Lett*. 1994;72(11):1666–1669. doi:10.1103/PhysRevLett.72.1666.
10. Evans CR, Coleman JS. Critical phenomena and self-similarity in the gravitational collapse of radiation fluid. *Phys Rev Lett*. 1994;72(12):1782–1785. doi:10.1103/PhysRevLett.72.1782.
11. Brańka AC, Heyes DM. Time correlation functions of hard sphere and soft sphere fluids. *Phys Rev E*. 2004;69(2):021202. doi:10.1103/PhysRevE.69.021202.
12. Kumar B, Evans GT. Translational dynamics in simple dense fluids. II. Self-diffusion. *J Chem Phys*. 1989;90(3):1812–1818. doi:10.1063/1.456023.
13. Sung W, Dahler JS. Two-fluid theory of coupled kinetic equations for a test particle and a background fluid. *J Chem Phys*. 1983;78(10):6264–6279. doi:10.1063/1.444592.
14. Evans GT. Translational and rotational dynamics of simple dense fluids. *J Chem Phys*. 1988;88(8):5035–5041. doi:10.1063/1.454684.
15. Evans GT. Momentum and stress relaxation in fluids illustrating caging. *J Chem Phys*. 2004;121(8):3667–3670. doi:10.1063/1.1772760.
16. Green MS. Markoff random processes and the statistical mechanics of time-dependent phenomena. II. Irreversible processes in fluids. *J Chem Phys*. 1954;22(3):398–413. doi:10.1063/1.1740082.
17. Mori H. Transport, collective motion, and Brownian motion. *Prog Theor Phys*. 1965;33(3):423–455. doi:10.1143/PTP.33.423.
18. Davis HT, Rice SA, Sengers JV. On the kinetic theory of dense fluids. IX. The fluid of rigid spheres with a square-well attraction. *J Chem Phys*. 1961;35(6):2210–2233. doi:10.1063/1.1732234.
19. McLaughlin IL, Davis HT. Kinetic theory of dense fluid mixtures. I. Square-well model. *J Chem Phys*. 1966;45(6):2020–2031. doi:10.1063/1.1727886.
20. Longuet-Higgins HC, Vallet JP. Transport coefficients of dense fluids of molecules interacting according to a square well potential. *Mol Phys*. 1958;1(3):284–294. doi:10.1080/00268975800100331.
21. Banaszak M, Chiew YC, Radosz M. Thermodynamic perturbation theory: Sticky chains and square-well chains. *Phys Rev E*. 1993;48(5):3760–3765. doi:10.1103/PhysRevE.48.3760.
22. Gil-Villegas A, Galindo A, Whitehead PJ, Mills SJ, Jackson G, Burgess AN. Statistical associating fluid theory for chain molecules with attractive potentials of variable range. *J Chem Phys*. 1997;106(10):4168–4186. doi:10.1063/1.473101.
23. Yu YX, Han MH, Gao GH. Self-diffusion in a fluid of square-well spheres. *Phys Chem Chem Phys*. 2001;3(3):437–443. doi:10.1039/b006807l.
24. Monnery WD, Mehrotra AK, Svrcak WY. Viscosity prediction from a modified square well intermolecular potential model. *Fluid Phase Equilib*. 1996;117(1–2):378–385. doi:10.1016/0378-3812(95)02975-3.
25. Nigra P, Evans GT. Stokes–Einstein relations for a square-well fluid. *J Chem Phys*. 2005;122(24):244508. doi:10.1063/1.1940032.